Resonant ultrasound spectroscopy of cylinders over the full range of Poisson's ratio

Tim Jaglinski and Roderic S. Lakes[a)]
Engineering Mechanics Program, Department of Engineering Physics, University of Wisconsin, Madison, Wisconsin 53706-1687, USA

(Received 28 October 2010; accepted 4 February 2011; published online 10 March 2011)

Mode structure maps for freely vibrating cylinders over a range of Poisson's ratio, ν, are desirable for the design and interpretation of experiments using resonant ultrasound spectroscopy (RUS). The full range of isotropic ν (–1 to +0.5) is analyzed here using a finite element method to accommodate materials with a negative Poisson's ratio. The fundamental torsional mode has the lowest frequency provided ν is between about –0.24 and +0.5. For any ν, the torsional mode can be identified utilizing the polarization sensitivity of the shear transducers. RUS experimental results for materials with Poisson's ratio +0.3, +0.16, and –0.3 and a previous numerical study for $\nu = 0.33$ are compared with the present analysis. Interpretation of results is easiest if the length/diameter ratio of the cylinder is close to 1. Slight material anisotropy leads to splitting of the higher modes but not of the fundamental torsion mode. © *2011 American Institute of Physics*. [doi:10.1063/1.3559305]

I. INTRODUCTION

Resonant ultrasound spectroscopy (RUS) allows the experimenter to determine elastic or viscoelastic moduli by measuring the resonance structure of various compact specimen geometries such as cubes, parallelepipeds, spheres, and cylinders. Typically, the sample is supported at two contact points by piezoelectric ultrasonic transducers; one for excitation and other for detection. Corners or edges provide weak elastic coupling to the transducers, hence minimally perturbing the vibration modes. Excessively strong coupling can shift the resonant frequencies and create parasitic damping. The RUS approach is simpler than other methods in that the specimen does not need to be glued, clamped, or aligned. The complexity of the method enters in the numerical procedure usually used to extract mechanical properties from the resonances.[1] Numerical inversion allows determination of all the elastic modulus tensor elements of an anisotropic material from the resonance spectrum. However, at least five resonant modes are typically required for each elastic constant to be found. If some modes are too weak to observe, the algorithm may not converge; the experimenter then may iteratively reposition the specimen, complicating the process. In materials of high damping, resonances are broad enough that higher ones overlap; the algorithm will not converge.

For isotropic materials it is expedient to study diagrams of modal frequency as a function of Poisson's ratio, commonly referred to as Demarest plots, for the purpose of experiment planning and interpretation. With such a plot, one can also extract moduli and damping simply without numerical inversion. Demarest provided the classic example for isotropic cubes[2] of Poisson's ratio between 0.05 and 0.45. A Demarest plot is useful in the following contexts. RUS is used to study the properties of materials that undergo solid state phase transformations. Mechanical damping increases in the vicinity of phase transformations,[3] broadening resonance peaks. Higher order modes then become difficult to resolve; therefore is helpful to be able to infer the stiffness moduli from a small number of low order modes. For example, it was impossible[4] to resolve peaks using a commercial RUS system if damping Q^{-1} exceeded 0.02. In this case 26–28 peaks were analyzed for an isotropic polycrystalline solid to obtain the shear and bulk moduli as well as the mechanical damping. Polymers and rocks also have sufficiently high damping that only the lowest modes can be resolved. A Demarest plot can aid mode location if some basic information about the specimen is known prior to the experiment to guide the experimenter to a smaller frequency window. In the context of numerical extraction of properties, a Demarest plot can guide the requisite initial guess used as input to the algorithm.

In addition to the Demarest plot for isotropic cubes, the modal structure for a solid sphere[5] was also determined analytically and has been plotted for Poisson's ratios between 0 and 0.5. To plot them a transcendental equation must be solved. A Demarest plot for a solid cylinder over a range of Poisson's ratio has not been presented, though modes for cylinders of length approximately equal to diameter (within 0.5%) were presented[6] for a single Poisson's ratio 0.33. Isotropic cylinders were also evaluated[7] using numerical inversion of resonance structure for up to ten modes. Moreover, a plot inclusive of the full range of isotropic Poisson's ratio is desirable since materials having negative Poisson's ratio have been developed.

In the present work, the mode structure for a short cylinder (length L equal to diameter D) is determined numerically and plotted for the full range of Poisson's ratio, ν, from –1 to 0.5. Results are compared to previous numerical analysis by others and with experimental results for materials of positive and negative Poisson's ratio. The effect of slight anisotropy and of variation of aspect ratio is also explored.

a)Author to whom correspondence should be addressed. Electronic mail: lakes@engr.wisc.edu.

II. NUMERICAL ANALYSIS

Cylindrical models were created using the commercial finite element code ABAQUS on a PC. For the mode structure as a function of Poisson's ratio ν, isotropic solid cylinders with varying length to diameter aspect ratios from 0.75:1 up to 2:1 were created using 3D, deformable solid models with ν varying from –0.999 to 0.5 by increments of about 0.1. The software accepts the full isotropic range of Poisson's ratio allowed by positive definite stability criteria (but neither $\nu = -1$, nor below). No symmetries were assumed in the modeling to avoid exclusion of asymmetric deformation modes. Swept meshes of reduced integration, quadratic 3D stress Hex dominated elemental meshes were applied from global seeds (with curvature control) of a minimum size of 0.06. All meshes contained around 5000 elements. Hex elements are hexahedral with 20 nodes per element; nodes are located at each corner and at the midpoint between adjacent corners. Mesh refinement shows that solutions converge using only a few hundred elements; a denser mesh was chosen to accurately visualize complicated mode shapes. For the isotropic case, a Young's modulus, E, of 70 GPa, Poisson's ratio of 0.3 and density of 2700 kg/m^3 were initially assumed, then the Poisson's ratio was varied. The shear modulus, G, was calculated through the usual isotropic relation $E = 2G(1 + \nu)$. To assess the effects of mild (5%) anisotropy, a number of materials were simulated with various combinations of the nine independent orthotropic engineering constants and are summarized in Table I. Mild anisotropy may occur in the processing of polycrystalline materials as in casting of metals. For the isotropic case, the elastic constants are independent of direction.

Mode shapes and frequencies were determined using the linear perturbation and frequency analysis module. Eigenvalues were computed using the Lanczos solver, with acoustic-structural coupling and an initial frequency shift of 40 Hz, the first 100 eigenvalues were retained for each cylinder. Computational time was less than 10 min for the first 100 eigenvalues.

III. EXPERIMENTAL

Samples were of circular cylindrical shape with length equal to the diameter. Samples were polymethyl methacrylate (PMMA) 25 mm in diameter, fused silica (amorphous SiO_2; Technical Glass, Painesville, OH) 9.95 mm in diameter and an open cell copper foam (Astro Met Associates, Inc., Cincinnati, OH). PMMA was cut from a rod, milled, and polished. Fused silica was cut from a rod with a diamond saw. The foam was processed by sequential plastic deformations of a cubical piece[8] to achieve a negative Poisson's ratio. This specimen was then shaped to a cylinder 26 mm in diameter by abrasive machining. Dimensions were measured with a micrometer; mass was determined with an analytical balance.

TABLE I. Orthotropic material models used in the anisotropic analysis.

Set	E_1[a]	E_2	E_3	ν_{12}	ν_{23}	ν_{13}	G_1[a]	G_2	G_3
Isotropic	70	70	70	0.3	0.3	0.3	(26.9)	26.9	26.9
1	70	70	70	0.3	0.3	0.3	26	26	24.7
2	70	70	70	0.3	0.3	0.3	24.7	26	26
3	70	70	70	0.3	0.3	0.3	27.3	26	24.7
4	70	73.5	66.5	0.3	0.3	0.3	26	26	26
5	70	70	70	0.3	0.285	0.315	26	26	26
6	70	73.5	66.5	0.3	0.285	0.315	27.3	26	24.7

[a]E and G are in units of GPa. The value for G in the isotropic case is calculated from E and ν and is shown in the parenthesis.

Transducers used were Panametrics V153 1.0/0.5 broadband shear, polarized with center frequency 1 MHz. The driver was excited via a synthesized function generator (Stanford Research DS 345). Shear transducers provide a stronger signal than compressional transducers for some modes, especially for the crucial fundamental torsion mode.[9] The output of the receiver transducer was amplified by a preamplifier with a bandpass of 100 Hz–300 kHz and gain from 100 to 1000. The function generator has a frequency resolution of 1 μHz, and an accuracy of 5 ppm. For low damping materials such as fused quartz, the resonant frequency can be resolved to within 1 Hz or about 5 ppm. For PMMA, which has high damping, frequency resolution was about one part per thousand. Better resolution could be achieved via longer averaging times or a lock-in amplifier but was not necessary for the purposes of this study. Signals were captured on a digital oscilloscope (Tektronix TDS 3012B); signal averaging over 16 cycles was used when appropriate to improve the ratio of signal-to-noise for polymer samples of high damping. Contact force was adjusted by moving one transducer with a fine micrometer drive (vertical stage, Newport type MVN50) and was reproduced among tests by measuring the feed-through signal at a frequency well below the lowest mode and reproducing that signal. Contact force can perturb modulus and damping measurement. The effect is usually small (0.1%) in the natural frequency and introduces a baseline damping that is pertinent in low damping materials. Contact force was controlled and minimized in these experiments, translating to a small systematic error. As for deviations from ideal dimensions, the effect is much less than the width of the data points for quartz and PMMA. The copper foam had a pore size of about 1/2 mm; its surface roughness limited the resolution of dimension measurement; mode splitting due to slight anisotropy exceeded any shift due to variance in dimensions.

The torsion mode was identified by rotating the specimen with respect to the direction of shear motion parallel to the transducer surface; this is the polarization direction. Specifically, referring to Fig. 1, alignment of the cylinder edge parallel to the polarization axis maximizes response for torsional modes; the orthogonal alignment produces a minimal response in torsion but a large response to other modes.

The torsion natural frequencies are given by

$$f = \frac{m}{2L}\sqrt{\frac{G}{\rho}}. \quad (1)$$

Here, f is the measured frequency in hertz, L is the sample length, G is the isotropic shear modulus, ρ is the sample density, and m is an integer. For the fundamental, $m = 1$. This frequency is the lowest one for short cylinders provided Poisson's ratio exceeds about –0.24.

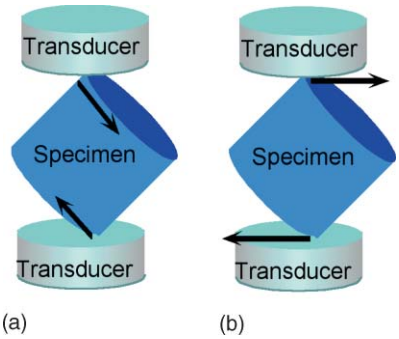

FIG. 1. (Color online) Schematic diagram of the RUS apparatus. (a) Polarization oriented for maximum response in torsion. (b) Polarization oriented for minimum response in torsion but maximum in bending or symmetric axial modes.

The shear modulus was determined by identification of the lowest torsion mode and use of Eq. (1) and Poisson's ratio was determined by aligning the observed mode structure with the Demarest plot. Numerical inversion was not used.

Damping was determined via $\tan\delta = (1/\sqrt{3})\,\Delta\omega/\omega_1$, in which ω_1 is the angular frequency at a resonance and $\Delta\omega$ represents the full width of the resonance curve at half maximum amplitude. This approximation is appropriate for $\tan\delta < 0.2$.

IV. RESULTS

A. Numerical results: Effect of Poisson's ratio on modes

A Demarest plot of the numerically determined mode structure is shown in Fig. 2. Frequencies are normalized to the first torsional mode. The modes shown in Fig. 2 are the first 20 modes calculated over a range of Poisson's ratio ν. Kinks in the curves are due to the discrete values of ν chosen. As can be seen, the present numerical results are in good agreement with those obtained by Senoo and Nishimura[6] for a cylinder with $\nu = 0.33$ and $L/D = 1.005$ (open triangles in Fig. 2 for a smaller number of modes). The Demarest plot shows that the fundamental mode of an isotropic cylinder is torsion for a range of Poisson's ratio from approximately –0.24 to +0.5. For $-0.24 < \nu < -0.7$, the fundamental mode is a predominantly bending mode (B1 in Fig. 2), transitioning to the first symmetric axial mode (SA in Fig. 2), for $\nu < -0.7$. The B1 mode has a sufficient slope with respect to Poisson's ratio to allow its determination; it is the second or third mode for $\nu > -0.24$. By contrast, in the cube, the first mode with much slope in Poisson's ratio is the fifth for $\nu > 0.25$. So the cylinder allows easier interpretation of elastic constants from the first few modes in comparison with the cube.

Representative mode shapes are shown in Fig. 3; the torsion mode shown as an inset in Fig. 2 is independent of Poisson's ratio ν. Minimum and zero displacement appears as dark blue in color online, and dark gray in black and white. Maximum displacements appear as red and medium gray, respectively; intermediate displacements are yellow, green, and light gray, respectively. For torsion, the maximum displacements occur at the cylinder edges in equal and opposite directions; zero displacements occur along the axis of rotation and on the surface at the midpoint between edges. For the SA, B1, S, and B2 modes shown in Fig. 3, motion occurs everywhere along the edges. For the S mode, a displacement minimum occurs in a region at the center of the curved surface. For the B1 mode, there are two displacement minima on the curved surface provided $\nu > -0.1$. The B2 mode exhibits minima on the curved

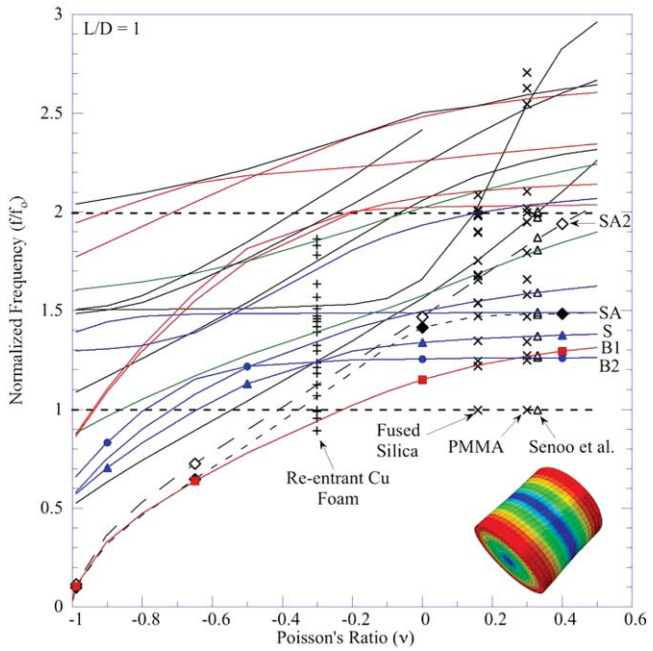

FIG. 2. (Color online) Demarest plot of the mode structure vs Poisson's ratio for an isotropic cylinder with length equal to diameter. The first 20 modes and their dependence upon ν are shown. Modal frequencies are normalized to the fundamental torsion frequency. Experimental points are indicated as (+) or (×). Calculations from Senoo *et al.* are shown as open triangles. SA (diamonds) refers to symmetric axial modes, or those dominated by bulk behavior over a range of Poisson's ratio, S (solid triangles) is a shear dominated mode, B1 (solid squares) is the lowest bending mode and B2 (solid circles) is a mixed mode. Only a few point shapes for each mode shape are shown to not obscure the data points. A representative mode shape for torsion is also shown.

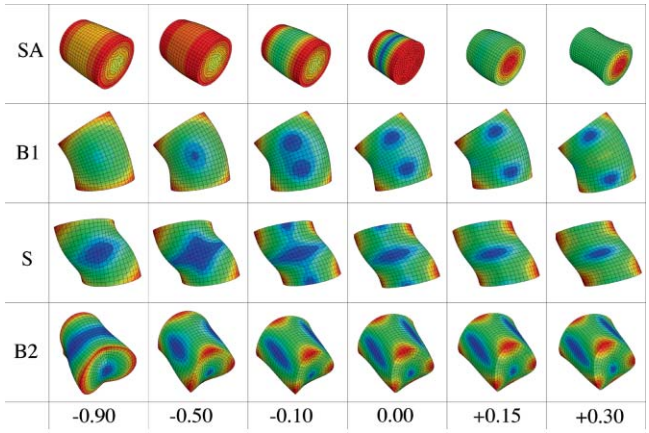

FIG. 3. (Color online) Representative mode shapes and their dependence on Poisson's ratio for the first few modes including the first symmetric axial mode (SA), the lowest bending mode (B1), a shear mode, (S) and a mixed mode (B2). All mode shapes shown are for cylinders with length equal to diameter. Colors represent magnitude of displacement; for interpretation of color (or shading), refer to the text.

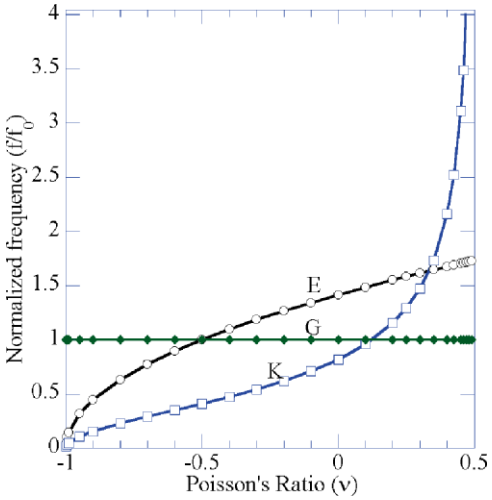

FIG. 4. (Color online) Behavior of modes that depend on ν. Normalized frequencies calculated for modes that depend on Young's modulus E, shear modulus G, or bulk modulus K.

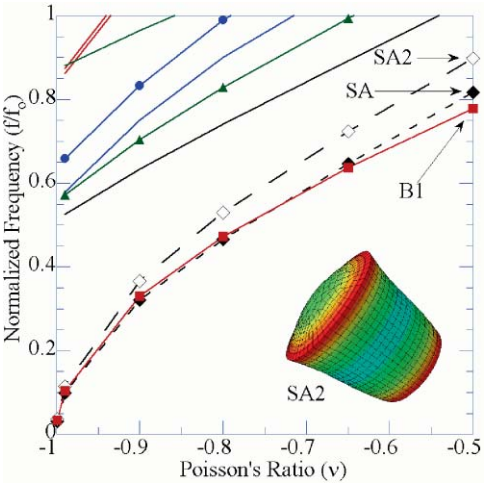

FIG. 5. (Color online) Mode frequencies normalized to the first torsional mode for a short cylinder, $L/D = 1$. The first bending mode (B1, solid squares) and the first (SA, solid diamonds) and second (SA2, open diamonds) symmetric axial modes show the greatest bulk dependence. The mode shape for SA2 ($\nu = 0.3$) is also shown; its appearance does not appreciably depend upon ν.

surface, and in the center of the flat end surface. While in the present work the torsion mode is identified via polarization sensitivity of shear transducers, it is also possible to discriminate among modes by placing compressional transducers at different locations on the specimen.

No modes are bulk dominated over the full range of Poisson's ratio as seen by comparing Fig. 2 with Fig. 4 which shows normalized frequencies versus Poisson's ratio

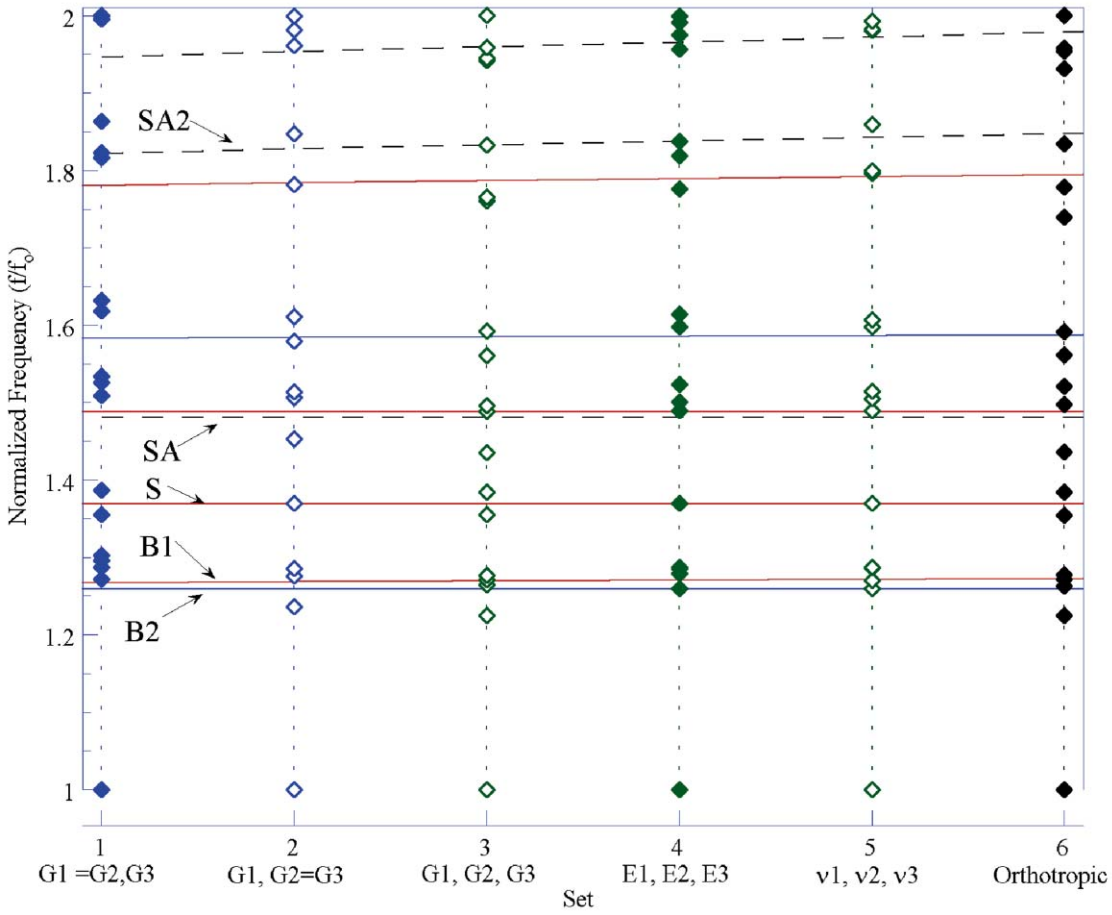

FIG. 6. (Color online) Effect of weak material anisotropy on mode structure (points). The 1-direction is along the cylinder's long axis. The mode structure is normalized to the fundamental torsional mode. Horizontal lines indicate the isotropic mode structure for $E = 70$ GPa and $\nu = +0.3$. For cases 4 and 5, $G_1 = G_2 = G_3$; for case 6, all nine material constants differ.

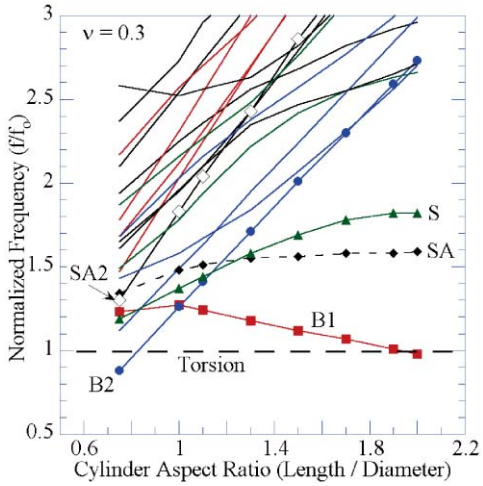

FIG. 7. (Color online) Effect of aspect ratio (length/diameter) on mode structure for an isotropic cylinder with a constant $\nu = 0.3$.

for modes that depend on shear modulus G, Young's modulus $E = 2G(1 + \nu)$ or bulk modulus $K = 2G(1 + \nu)/3(1 - 2\nu)$. The region for Poisson's ratio tending to –1 is of interest in the context of stability of materials that undergo phase transformations in which the bulk modulus softens. Behavior of bulk type (K) and bending type (E) modes is similar as $\nu = -1$ is approached. Modes for the short cylinder normalized to the fundamental torsion frequency include several that tend to zero for small Poisson's ratio tending to –1 (Fig. 5), hence are bulk dominated in that regime. The lowest bending mode (B1) has a bending character for all Poisson's ratio; indeed the dependence on Poisson's ratio reveals behavior dominated by Young's modulus E. The shear mode (S) frequency is essentially independent of Poisson's ratio for positive ν; because it shows some sensitivity for negative ν, it is not purely shear. Modes, which depend only on G, have a constant value in a Demarest plot since all frequencies are normalized to the first torsion mode which depends only on G. The first SA mode acquires a volumetric character for negative Poisson's ratio; indeed in that regime it is sensitive to the bulk modulus. For positive ν there is substantial shear in this mode as indicated by nonuniform shape change, specifically large lateral contraction near the center of the curved surface relative to the ends of the cylinder. The mixed mode (B2) has a complex shape but is shear dominated for positive ν. The second symmetric axial (SA2) mode, shown as an inset in Fig. 8(a), has a shape suggestive of plate bending; it is sensitive to ν, but for positive ν it has a relatively high frequency.

B. Numerical results: Effect of material anisotropy on mode structure

Several cases of material anisotropy (Table I) were examined to determine their effect on the mode structure of orthotropic short cylinders. Shear moduli, Young's moduli and Poisson's ratio were independently perturbed 5% from the isotropic form. It was found that splitting of the fundamental torsional mode does not occur but higher modes are split for orthotropic short cylinders as shown in Fig. 6. Similarly the solution for spheres reveals no splitting of the lowest mode, but cylinders are usually easier to fabricate than spheres. By contrast, the torsional mode for cubes and parallelepipeds is split into two resonance peaks. Hence, even in the presence of slight anisotropy, short cylinders are an amenable geometry, coupled with shear polarized transducers, to quickly identify the torsional mode and to infer the shear modulus $G = 2[C_{55}^{-1} + C_{66}^{-1}]^{-1}$ for any Poisson's ratio without the need for computer inversion.

C. Numerical results: Effect of aspect ratio

The effect of aspect ratio (the ratio of length to diameter L/D) on modes for a Poisson's ratio of 0.3 is shown in Fig. 7. The lowest mode is torsional for L/D between about 0.87 and 1.94. Small deviations from $L/D = 1$ have the following effect on the form of the fundamental vibrational mode. A 1% increase in length decreases the frequency of the fundamental torsion mode by 1% and increases the ratio between the frequencies of the first torsional and bending

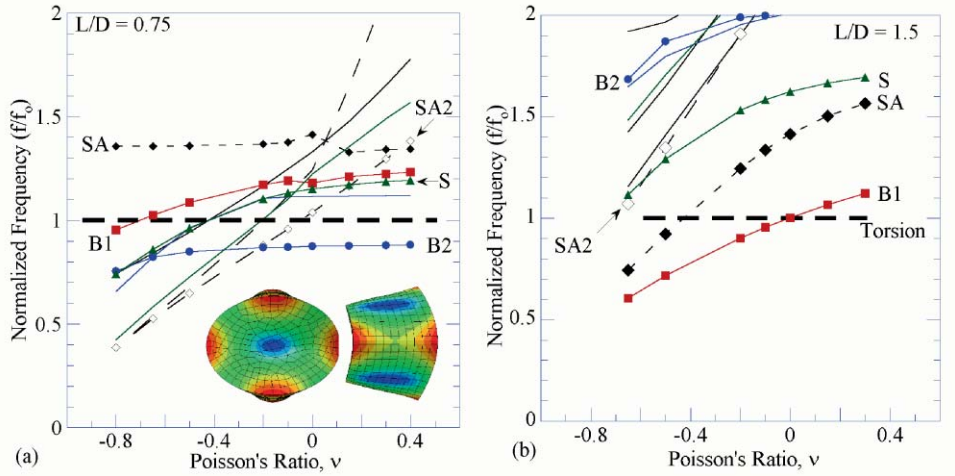

FIG. 8. (Color online) Dependence of the first few modes upon ν for isotropic cylinders with aspect ratios of (a) 0.75 and (b) 1.5. Alternate orthogonal views of the B2 mode shape from Fig. 3 are shown in (a).

TABLE II. Values of material properties inferred from the torsional modes.

Material	Diameter (mm)	Length (mm)	L/D	Density, ρ (g/cc)	ν	f_{torsion} (kHz)	G (GPa)	tan δ
PMMA	25.54	25.40	0.995	1.2	0.3	26.8	1.9	2.2×10^{-2}
SiO_2	9.96	9.95	0.999	2.2	0.16	189.8	31.4	4.7×10^{-4}
Cu foam	25.5	25.5	1	0.514	–0.3	5.03	0.12	3×10^{-4}

modes, $f_{\text{torsion}}/f_{\text{bending}}$ by less than 1%. For $\nu = 0.3$, the effect of small variations in aspect ratio do not greatly perturb the relative order of the first few modes below the second torsional harmonic. Some authors prefer elongated specimens ($L/D \geq 2.5$) for rock cylinders[10] to be interpreted via numerical algorithms, so the lowest mode is bending, with some sensitivity to the longitudinal wave speed. These rock specimens were anisotropic.

The effect of aspect ratio for a range of Poisson's ratio is shown in Fig. 8. For $L/D = 0.75$, the lowest mode is a mixed shear mode with a slight dependence on Poisson's ratio for $\nu > -0.4$, as shown in Fig. 8(a). For $L/D = 1.5$, the lowest mode is torsional for $\nu > -0.05$; the second mode in that range is bending. The bending mode is sufficiently close to the torsion one for Poisson's ratios associated with common materials that interpretation would be difficult for high damping materials. By contrast, the mode structure for $L/D = 1$, Fig. 2, is more favorable for interpretation because the torsional mode is the lowest one for $\nu > -0.24$ and is well separated from the others for $\nu > 0$, allowing immediate extraction of the shear modulus and its damping. Moreover, after the shear modulus is determined from the torsion mode, the bending mode provides a good measure of Poisson's ratio over its full range.

D. Experimental results

Experimentally determined mode structure for the PMMA, SiO_2, and Cu foam cylinders are plotted in comparison with the numerical results in Fig. 2. Table II contains the measured frequencies and inferred shear moduli from the torsional modes. Modes were verified as torsional by the polarization sensitivity with respect to the shear transducer orientation. Cylinders were rotated 90° from the shear polarization direction and the response amplitude decreased dramatically for the torsion modes. No modes below the torsion fundamental were observed for PMMA and SiO_2. An instrumental resonance near or below 1 kHz was easily recognized by its low frequency and broad response. The shear modulus inferred from Eq. (1) for PMMA, 1.9 GPa, is consistent with reported values at ultrasonic frequencies and about twice the modulus observed at quasistatic low frequency; the modulus for SiO_2 is also consistent with literature values. Matching the obtained frequencies with the numerically determined mode structures gives Poisson's ratios of +0.3 and +0.16 for PMMA and SiO_2, respectively, again reasonable for these materials. It is notable that use of the Demarest plot allows extraction of the modulus and Poisson's ratio of PMMA even though the damping (determined via resonant peak width measurement) is sufficiently high that some higher resonances overlap, which would preclude a numerical inversion. Indeed, Demarest suggested that G be extracted from a cube mode independent of Poisson's ratio, then to extract Poisson's ratio from one or more higher modes.

As for the copper foam specimen, the torsional resonant frequency was 5.03 kHz, similarly verified as torsion; the shear modulus was calculated to be 120 MPa, reasonable in view of the density. However, the torsional mode was not the fundamental mode for this material. A nontorsional mode, identified as such since it was observed in both polarizations, occurred at a lower frequency than the torsional mode. The Poisson's ratio of the re-entrant copper foam was determined to be about –0.3 as shown in the mode structure of Fig. 2. Some splitting of the first mode as well as higher modes was observed and is attributed to a slight anisotropy, reducing the precision in inferring Poisson's ratio. The damping of copper foam was about 3×10^{-4}.

V. CONCLUSIONS

A Demarest plot of mode frequency versus Poisson's ratio ν was generated numerically. The fundamental mode for a short cylinder with length equal to diameter ($L = D$) transitions from torsion to bending for $\nu = -0.24$ and then a symmetric axial, or bulklike, mode for $\nu < -0.7$. The present numerical results are in good agreement with previous calculations (for $\nu = 0.33$) and present RUS experiments for cylinders with negative and positive Poisson's ratios. A negative Poisson's ratio for the Cu foam was inferred from the modal structure by identification of a mode below the torsional by virtue of the fact a lower mode was detected in both shear polarizations. For the other cylinders, no modes below the fundamental torsion were detected.

Small (5%) material anisotropies do not split the fundamental torsion mode for short cylinders and spheres, but do split the fundamental for cubes and parallelepipeds. This was also observed in the Cu foam as a splitting in modes other than the torsional; the splitting did not interfere with interpretation.

As for aspect ratio, deviations from $L = D$ of 1% shift the resonant frequency by only 1%. A 10% deviation does not greatly perturb the relative order of the modes up to the first torsional harmonic (for $\nu = 0.33$). Short cylinders with $L/D = 1$ are favorable for interpretation because the torsional mode is the lowest one, well separated from the others for $\nu > 0$, allowing immediate extraction of the shear modulus and its damping. In this case bending is the second or third mode, with sufficient slope to readily extract Poisson's ratio.

[1]W. M. Visscher, A. Migilori, T. M. Bell, and R. A. Reinert, J. Acoust. Soc. Am. **90**, 2154 (1991).
[2]H. H. Demarest, Jr., J. Acoust. Soc. Am **49**, 768 (1971).

[3]J. I. Perez-Landazabal, V. Recarte, D. S. Agosta, V. Sanchez-Alarcos, and R. G. Leisure, Phys. Rev. B **73**, 224101 (2006).
[4]M. A. Carpenter, A. Buckley, P. A. Taylor, and T. W. Darling, J. Phys. Condens. Matter **22**, 035403 (2010).
[5]A. Yaoita, T. Adach, and A. Yamaji, NDT & E Int. **38**, 554 (2005).
[6]M. Senoo, T. Nishimura, and M. Hirano, Bull. JSME **27**, 2339 (1984).
[7]P. Heyliger, A. Jilani, H. Ledbetter, R. G. Leisure, and C. L. Wang, J. Acoust. Soc. Am. **94**, 1482 (1993).
[8]E. A. Friis, R. S. Lakes, and J. B. Park, Negative Poisson's ratio polymeric and metallic materials, J. Mater. Sci. **23**, 4406 (1988).
[9]Y. C. Wang and R. S. Lakes, Rev. Sci. Instrum. **74**, 1371 (2003).
[10]B. J. Zadler, J. H. L. Le Rousseau, J. A. Scales, and M. L. Smith, Geophys. J. Int. **156**, 154 (2004).